

STUDYING INDIVIDUAL VIRUSES AND BACTERIA WITH NANOFLUIDICS

Zachary D. Harms¹, Laurence Kohler¹, Seth M. Madren¹, Joshua D. Baker¹, Lisa Selzer²,
Adam Zlotnick², David T. Kysela³, Yves V. Brun³, and Stephen C. Jacobson^{1*}

¹Department of Chemistry, ²Department of Molecular and Cellular Biochemistry, and
³Department of Biology, Indiana University, Bloomington, IN 47405 USA

ABSTRACT

We are developing instrumentation and methods to study individual viruses and bacteria. For the virus studies, we are fabricating nanochannels with multiple pores in series for resistive-pulse sensing of hepatitis B virus (HBV) capsids. With two or more pores in series, single particles are interrogated multiple times to improve measurement of particle sizes and to determine their electrophoretic mobilities. For the bacteria studies, we are using nanochannel arrays to trap bacteria and track cell growth and aging over multiple generations. Confinement of bacterial growth in one dimension permits epigenetic inheritance studies from parent and child.

KEYWORDS: nanofluidics, nanochannel, resistive-pulse sensing, virus, bacteria

EXPERIMENTAL

For the resistive-pulse sensing experiments, we fabricate two V-shaped microchannels in a glass substrate by conventional techniques, then nanochannels with integrated nanopores are milled with a focused ion beam (FIB) instrument into the substrate to span the microchannels (see Figure 1). Use of an electron flood gun minimizes surface charging by the ion beam during the mill and circumvents the need to coat the substrates with a metal film. Nanopores are typically 50-nm wide and 50-nm deep and match the sizes of the 31-nm diameter T = 3 HBV capsid and 36-nm diameter T = 4 HBV capsid. Potentials between 100 and 1000 mV are applied across the nanochannel to drive the capsids through the pores, and the resulting current signal is amplified and digitized for analysis.

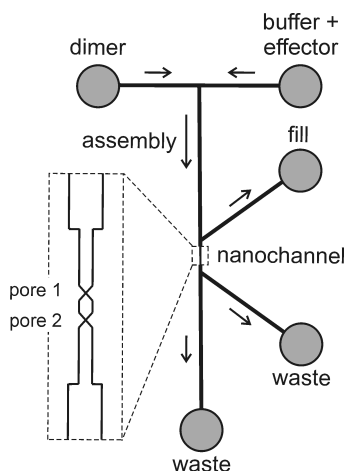


Figure 1. Schematic of a nanofluidic device for resistive-pulse sensing of HBV capsids. The two V-shaped microchannels are bridged by a nanochannel that has two nanopores in series. Inset is an expanded view of the nanochannel with pores 1 and 2 spaced 2.5 μm apart.

To track individual bacteria, arrays of nanochannels for the cell trapping device are cast in poly(dimethylsiloxane) (PDMS) from a master written in the negative-tone resist SU-8 by electron-beam (e-beam) lithography. The height of the nanochannel master is controlled by the e-beam resist thickness (e.g., 0.5 to 2 μm thick), and the width of the nanochannel master is defined by the scanning electron microscope (SEM) used to pattern the nanochannels. By varying the write area of the e-beam, a range of channel widths (e.g., 200, 300, 400, and 500 nm) are exposed to ensure cells are adequately trapped. The e-beam lithography step is repeated to generate a 4 \times 4 grid, resulting in over 1200 parallel nanochannels to trap cells. After fabrication of the nanochannel master, microfluidic channels are formed perpendicular to the nanochannel arrays in order to distribute buffers and reagents to the nanochannel arrays. The replicas of the fluid layers in the PDMS are then integrated into a three-layer device (control layer, fluid layer, and glass coverslip) to automate the cell loading and trapping (see Figure 2). Pressure applied through the control layer above the nanochannel array is actuated to trap and release cells.

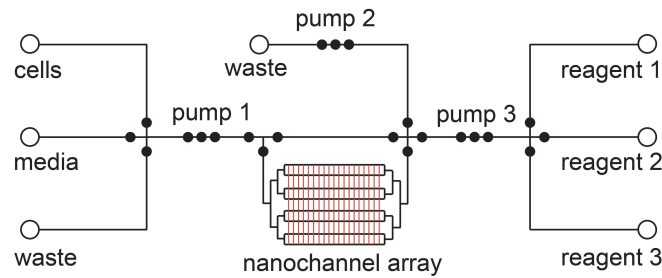


Figure 2. Schematic of the programmable microfluidic device with an integrated nanochannel array for monitoring aging of single cells over multiple generations. Open circles represent reservoirs, and closed circles represent valves. Three valves in series are used as peristaltic pumps and are labeled pumps 1, 2, and 3. A large open region in the control channel above the nanochannel array actuates the trapping region.

RESULTS AND DISCUSSION

To sense viruses and measure their assembly, we need a technique that is able to make measurements in solution, with single particle sensitivity, in real time, at biologically relevant concentrations, and without the use of chemical labels. Resistive-pulse sensing meets these criteria by measuring the change in conductivity as a particle transits a nanofluidic pore of comparable dimensions. Fabrication of nanopore devices in-plane permits us to arrange nanochannels in any arbitrary format and systematically evaluate nanopore dimensions (e.g., cross-section and length) and pore-to-pore spacing for optimized particle characterization.

For the resistive-pulse measurements, HBV capsids are electrokinetically driven through the nanochannel, and as a capsid transits a pore, a decrease in current (pulse) is observed. With two pores in series, two current pulses are detected [1]. Figure 3 shows that pulse amplitude for the current pulses increases with increasing potential, whereas pulse width and pore-to-pore transit time decrease. The pulse amplitude is proportional to the particle size, and the pore-to-pore transit time is used to calculate capsid velocity, and subsequently, electrophoretic mobility of the capsid. Another advantage of the resistive-pulse sensing technique is the ability to discriminate between small changes in particle size. A 5-nm difference in HBV capsid diameter is easily resolved in mixed populations of the T=3 and T=4 HBV capsids.

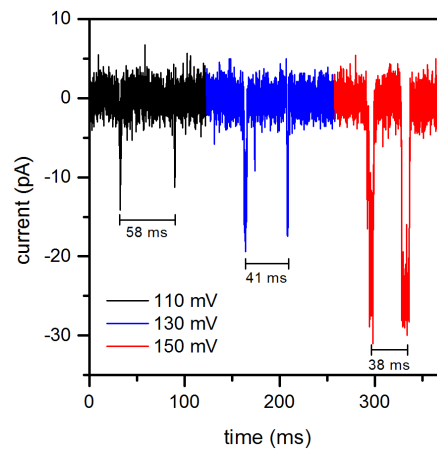


Figure 3. Variation of current with time for resistive-pulse sensing of hepatitis B virus (HBV) capsids transiting through two nanopores in series with 110, 130, and 150 mV applied. Each HBV capsid generates two current pulses while transiting the two nanopores.

For the bacteria growth and aging studies, the nanochannels trap the bacteria and permit growth in one dimension [2], and microchannels provide fresh media to the bacteria and flush away cells that escape the nanochannels. The nanochannels must closely match the widths of the bacteria in order to immobilize the cells without the application of physical stress to the trapped cells. To create a device that traps cells of different sizes, the nanochannel array contains nanochannels with a range of widths. The nanochannels must also be deep enough to permit diffusion of fresh media into the nanochannels, yet shallow enough to confine the cells in the z-dimension. The SU-8 masters contained raised features that were 1.3- μm tall and had widths of 200, 300, 400 and 500 nm.

The distance between the microchannels determines the length of the nanochannels. Longer nanochannels trap cells for more generations before they are pushed out of the nanochannels by the growth of neighboring cells. However, as the nanochannel lengthens, the force required to push cells out of the nanochannel and into the microchannel increases. If the force required to push the cells into the microchannel is too large, the cells are stressed as they push against each other in the nanochannel and filament. Also, the cells will push under the PDMS and will no longer be contained by the

nanochannels. We have determined that a nanochannel length up to 140 μm confines the bacteria for multiple generations without the loss of confinement or excessive stress to the cells.

To confirm that the device could be used to trap bacteria without perturbation of their growth over time, *B. subtilis* was trapped in the nanochannels, and images were collected from multiple positions in the nanochannel array for 10 h. Individual cells were tracked throughout the experiment to observe division times and to create a lineage. Such lineages are a powerful tool to observe epigenetic inheritance as well as cellular aging and differentiation. A concern associated with nanochannels formed in PDMS is that the cells in the nanochannels may deplete nutrients faster than they can diffuse into the nanochannel. To determine if nutrient depletion occurs in the nanochannel array, the division time of the trapped bacteria before the nanochannels were filled with cells was compared to the division time after the nanochannels were completely filled with cells (Figure 4). There is no statistical difference in the division time of *B. subtilis* before the nanochannels are filled ($55 \text{ min} \pm 25 \text{ min}$) and the division time after the nanochannels are filled ($55 \text{ min} \pm 20 \text{ min}$). Moreover, division times in the nanochannel arrays are comparable to those observed in standard assays.

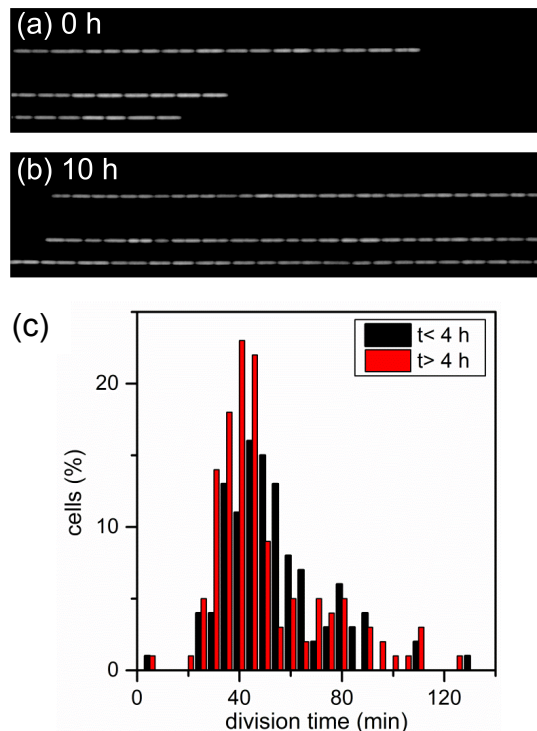


Figure 4. Fluorescence images of *B. subtilis* (a) at the start of the experiment and (b) after 10 h of growth in the nanochannel array. (c) Distribution of division times for *B. subtilis* cells trapped in the nanochannel array before the nanochannels are filled with cells ($t < 4 \text{ h}$) and after the nanochannels are filled with cells ($t > 4 \text{ h}$).

ACKNOWLEDGEMENTS

This work is supported in part by the Lilly Endowment, Inc. and NIH ROI GM100071. The authors thank the Indiana University Nanoscale Characterization Facility for use of its instruments.

REFERENCES

- [1] Z.D. Harms, K.B. Mogensen, P.S. Nunes, K. Zhou, B.W. Hildenbrand, I. Mitra, Z. Tan, A. Zlotnick, J.P. Kutter, and S.C. Jacobson, "Nanofluidic Devices with Two Pores in Series for Resistive-Pulse Sensing of Single Virus Capsids," *Anal. Chem.* 83, 9573-9578, 2011.
- [2] J.R. Moffitt, J.B. Lee, and P. Cluzel, "The Single-Cell Chemostat: An Agarose-Based Microfluidic Device for High-Throughput Single-Cell Studies of Bacteria and Bacterial Communities," *Lab Chip*, 12, 1487-1494, 2012.

CONTACT

*Stephen C. Jacobson; tel: +1-812-855-6620; jacobson@indiana.edu